Antineoplastic Agents. 379. Synthesis of Phenstatin Phosphate[1a,†]

George R. Pettit,* Brian Toki, Delbert L. Herald, Pascal Verdier-Pinard,[1b] Michael R. Boyd,[1b] Ernest Hamel, and Robin K. Pettit

Cancer Research Institute and Department of Chemistry, Arizona State University, Tempe, Arizona 85287-1604

Received September 25, 1997

A structure−activity relationship (SAR) study of the South African willow tree (*Combretum caffrum*) antineoplastic constituent combretastatin A-4 (**1b**) directed at maintaining the (*Z*)-stilbene relationship of the olefin diphenyl substituents led to synthesis of a potent cancer cell growth inhibitor designated phenstatin (**3b**). Initially phenstatin silyl ether (**3a**) was unexpectedly obtained by Jacobsen oxidation of combretastatin A-4 silyl ether (**1c** → **3a**), and the parent phenstatin (**3b**) was later synthesized (**6a** → **3a** → **3b**) in quantity. Phenstatin was converted to the sodium phosphate prodrug (**3d**) by a dibenzyl phosphite phosphorylation and subsequent hydrogenolysis sequence (**3b** → **3c** → **3d**). Phenstatin (**3b**) inhibited growth of the pathogenic bacterium *Neisseria gonorrhoeae* and was a potent inhibitor of tubulin polymerization and the binding of colchicine to tubulin comparable to combretastatin A-4 (**1b**). Interestingly, the prodrugs were found to have reduced activity in these biochemical assays. While no significant tubulin activity was observed with the phosphorylated derivative of combretastatin A-4 (**1d**), phosphate **3d** retained detectable inhibitory effects in both assays.

The African willow tree *Combretum caffrum* Kuntze (Combretaceae) proved to be a very productive source of cancer cell growth (murine P388 lymphocytic leukemia) inhibitory stilbenes, bibenzyls, and phenanthrenes.[2] Since 1979, we have been pursuing promising leads and have focused on the three most active (inhibition of cancer cell growth and polymerization of tubulin)[2] constituents, namely combretastatin A-1 (**1a**), A-2 (**2**), and A-4 (**1b**) (Chart 1).[2] Of these, combretastatin A-4 (**1b**) has reached the most advanced stage of preclinical development as the soluble prodrug (**1d**). Meanwhile other research groups have also been extending structure−activity relationships (SAR) among the combretastatins[3] and related stilbenes.[4]

One of the clearest conclusions from SAR studies in our laboratories is the cancer cell growth inhibition requirement for *Z*-geometry in the A-series of combretastatin stilbenes.[2] With the corresponding (*E*)-stilbenes, the cancer cell growth inhibitory and antitubulin activity drops precipitously from that exhibited by the corresponding *cis*-isomers. This observation suggested the possibility that other potentially useful structural modifications might be of interest, in which the *cis*-diaryl relationship is preserved by the simple conversion of the bridging olefin unit of, for example, combretastatin A-4 (**1b**) to epoxide- or cyclopropyl-type derivatives. However, subjection of combretastatin A-4 silyl ether (**1c**)[2] to a variety of oxidation procedures, such as *m*-chloroperbenzoic acid, sodium periodate,[5] and *N*-bromoacetamide followed by potassium carbonate, resulted in complex mixtures of products whose components were difficult to isolate.

An attempted epoxidation of combretastatin A-4 silyl ether[2a] (**1c**) using the Jacobsen chiral Mn (salen) complex[6a] resulted in rearrangement and oxidation products (indicated by ^{1}H NMR and TLC analyses). Use of protecting groups for the phenol offered no improvement, and the absence of a protecting group resulted in apparent polymerization. Rearrangements of epoxides have been studied extensively by Cope and others.[7] Pertinent here is the observation that *cis*- and *trans*-stilbene epoxides rearrange under basic conditions to form deoxybenzoin and diphenylacetaldehyde, respectively, via migration of a phenyl group. Conversely, in an acidic environment, *p*-methoxystilbene oxide has been shown to undergo S_Ni displacement followed by a possible migration. Furthermore, certain transition metals such as titanium can serve as catalysts for catalytic rearrangement of epoxides.

In the case of combretastatin A-4, formation of the oxirane by the Jacobsen oxidation was observed by ^{1}H NMR, but the compound resisted isolation. In addition, the derived 1,1-diphenylacetaldehyde and benzophenone (**3a**) products appeared to be formed. Following isolation of silyl ether **3a** (10% yield) and mass spectral analysis of the suspected benzophenone, cleavage of its silyl ether protective group showed the loss of one carbon atom (**3b**). A conjugated carbonyl peak at 1633 cm^{-1} was seen in the IR spectrum. Loss of the olefin bridge was established by NMR. This result suggested the need for structure confirmation of ketone **3b** by X-ray crystallography, which demonstrated the compound was indeed 3-hydroxy-3′,4,4′,5′-tetramethoxybenzophenone (Figure 1). Since Jacobsen's epoxidation was performed under basic conditions, formation of the presumed (by NMR) oxirane intermediate was apparently followed by an aryl shift (Scheme 1) to form the corresponding diarylacetaldehyde (evident by ^{1}H NMR) by rearrangement. Finally, oxidative cleavage would give the silylated benzophenone (**3a**).

Because of the potent cancer cell line growth inhibition displayed by the resultant deprotected benzophenone, it was designated phenstatin. The structure of phenstatin (**3b**) (Chart 1) proved to be closely related to the aromatic system of podophyllotoxin **5**, the target of our attempts,[8] beginning in 1958, to locate the

† Dedicated to the memory of Dr. Kenneth D. Paull, 1942−1998.

S0022-2623(97)00644-4 CCC: $15.00 © 1998 American Chemical Society
Published on Web 04/21/1998

Chart 1

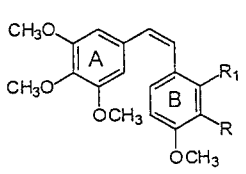

1a, R = OH, R_1 = OH
Combretastatin A-1
1b, R = OH, R_1 = H
Combretastatin A-4
1c, R = $OSi(CH_3)_2C(CH_3)_3$, R_1 = H
1d, R = $OP(O)(ONa)_2$, R_1 = H
Combretastatin A-4 prodrug
1e, R = R_1 = H

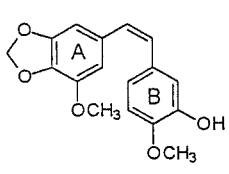

2, Combretastatin A-2

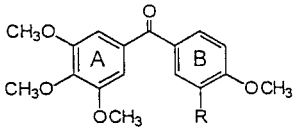

3a, R = $OSi(CH_3)_2C(CH_3)_3$
3b, R = OH, Phenstatin
3c, R = $OP(O)(OCH_2C_6H_5)_2$
3d, R = OP(O)(OH)(ONa)
Phenstatin prodrug
3e, R = $OCOCH_3$
3f, R = H

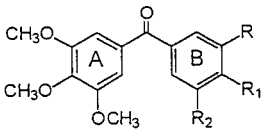

4a, R = H, R_1,R_2 = OCH_2O
4b, R = R_2 = CH_3, R_1 = H
4c, R = H, R_1 = R_2 = OCH_3
4d, R = R_2 = OCH_3, R_1 = H
4e, R = R_2 = Cl, R_1 = H
4f, R = R_2 = F, R_1 = H

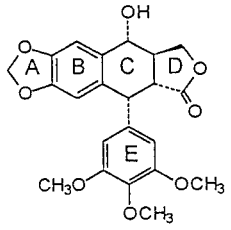

5

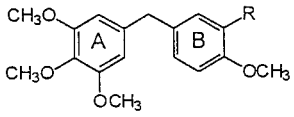

7a, R = OH
7b, R = H

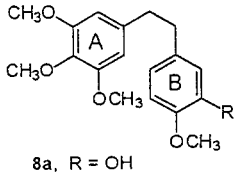

8a, R = OH
8b, R = H

structural core responsible for the antineoplastic activity of this important lignan.

To improve the availability of phenstatin by a more efficient synthesis, we explored several shorter routes. The general procedure we reported[8] in 1962 for obtaining ketone **4a** based on a morpholine amide intermediate proved to be most effective. The phenstatin amide precursor was prepared from 3-[(*tert*-butyldimethylsilyl)oxy]-4-methoxybenzaldehyde by oxidation to the corresponding carboxylic acid using potassium permanganate, followed by conversion to the acid chloride, and finally treatment with morpholine (Scheme 2). The amide **6a** was allowed to react with the lithium derivative prepared from 3,4,5-trimethoxybromobenzene[9] and *tert*-butyllithium at −78 °C followed by deprotection to afford phenstatin (**3b**) in 30% overall yield. Similarly, a series of related benzophenones (**4**) were synthesized for SAR purposes (Table 1).

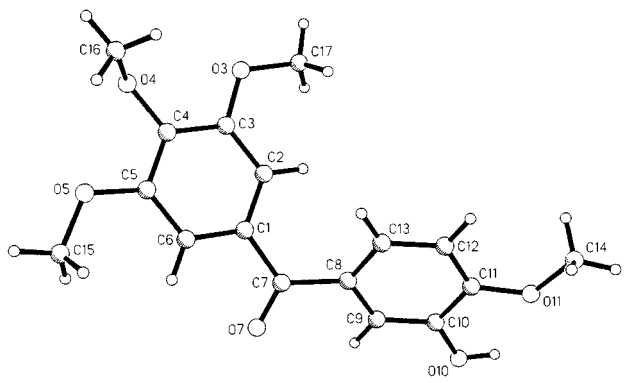

Figure 1. Computer-generated perspective drawing of phenstatin (**3b**).

Because of the improved therapeutic effects of the combretastatin A-4 sodium phosphate (**1d**) prodrug[10] vs the parent phenol (**1b**),[11] the corresponding phenstatin prodrug (**3d**) was synthesized (**3b** → **3d**, Scheme 3). We have used both of the previous phosphorylation techniques[10,12] for such syntheses, based on pentavalent and trivalent phosphorus precursors. However, they have proven to be substantially less effective than employment of the dibenzyl phosphite approach.[13] The prodrug was synthesized in three steps from phenstatin via phosphorylation of phenol **3b** employing dibenzyl phosphite (under basic conditions in 1:1 acetronitrile−DMF),[13] followed by cleavage of the benzyl groups (**3c**) via catalytic hydrogenolysis[12] and reaction of the phosphoric acid product with sodium methoxide in methanol to afford sodium phosphate prodrug **3d** in 56% overall yield.

Compounds **3b**,**d**, **1d**, and **4a**−**f** were comparatively evaluated in the NCI 60 cell line human tumor

Scheme 1. Oxidation of Combretastatin A-4 Silyl Ether (**1c**) to Phenstatin Silyl Ether (**3a**)

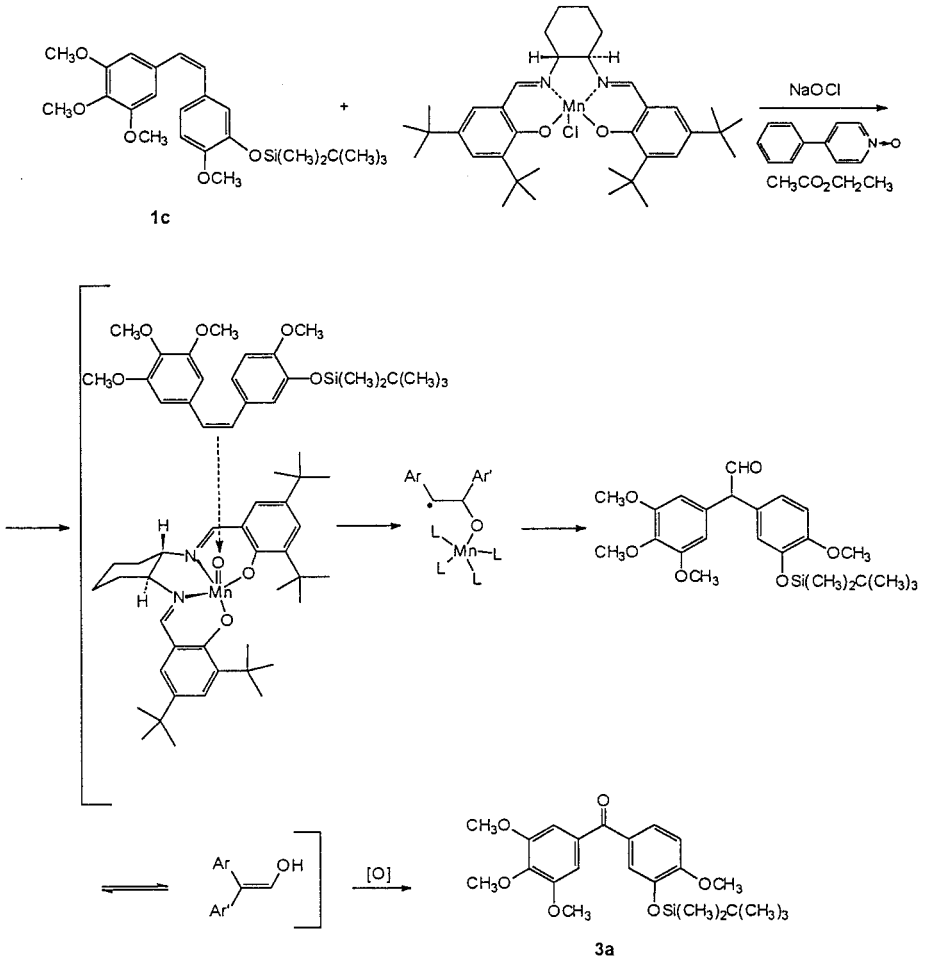

Scheme 2

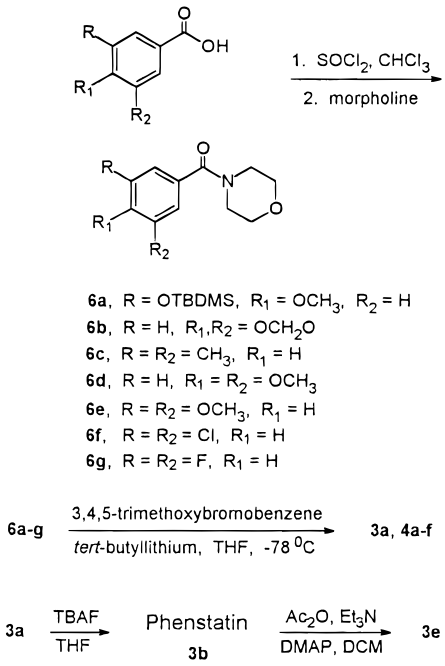

screen.[16−20] As illustrated in Table 2, the water-soluble phenstatin phosphate prodrug (**3d**) and the parent phenstatin (**3b**) were essentially indistinguishable in potency (e.g., mean panel GI_{50} values) and differential cytotoxicity profiles (e.g., compare correlation coefficients). Moreover, **3b**,**d** were quite similar to the combretastatin A-4 phosphate prodrug (**1d**) in terms of both potency and differential cytotoxicity. In contrast, the related benzophenones (**4a**−**f**) were generally much less potent than **3b,d** or **1d**, although their differential cytotoxicity profiles (and therefore their presumed mechanism of action[20]) did not differ remarkably from that of the lead compound. Interestingly, the acetate derivative (**3e**) of phenstatin exhibited significant human cancer cell line inhibitory activity: e.g., CNS U251 GI_{50} 0.0039 μg/mL, pharynx FADU GI_{50} 0.0055 μg/mL, and prostate DU-145 GI_{50} 0.0029 μg/mL. Like combretastatin A-4 (**1b**),[2a] phenstatin (**3b**) inhibited growth of the Gram-negative pathogenic bacterium *Neisseria gonorrhoeae* (minimum inhibitory concentration 50−100 μg/disk). At 100 μg/disk, neither phenstatin prodrug (**3d**) nor the acetate derivative (**3e**) were active against *N. gonorrhoeae*.

Because of the known potent interactions of combretastatin A-4 (**1b**)[2] and ketone **3f**[3f] with the colchicine site of tubulin and because of COMPARE[16−18,20] studies, such as those presented in Table 2, suggesting similar mechanisms of action, phenstatin (**3b**), its prodrug **3d**, and compounds **4a**−**f** were evaluated for potential inhibitory effects on tubulin polymerization and on the binding of colchicine to tubulin (Table 4). Simultaneous studies were performed for comparison of the new compounds with combretastatin A-4 (**1b**), its prodrug **1d**, and the related compounds **3f**,[3f] **1e**,[3h] **7a**,[3g] **7b**,[3f] **8a**,[3g] and **8b**[3h] (Chart 1).

Table 1. Physical Properties of the Amides and Benzophenones

compd	% yield (from **5**)	cryst solvent	mp (°C)	formula[c]
6a	94	hexane	66−67	$C_{18}H_{29}NO_4Si$
6b	88	*a*	87−88	$C_{13}H_{17}NO_2$
6c	73	*a*	78−79	$C_{13}H_{17}NO_4$
6d	78	*a*	84−85	
6e	97	*a*	78−79	$C_{13}H_{17}NO_4$
6f	100[f]	*a*	117−119	$C_{11}H_{11}Cl_2NO_2$
6g	97[f]	*b*	68−70	$C_{11}H_{11}F_2NO_2$
3a	76	hexane	74−75	$C_{23}H_{32}O_6Si$
3b	83	ethyl acetate−hexane	149−150	$C_{17}H_{18}O_6$
3c	72[d]	n/a	clear oil at rt	$C_{31}H_{31}O_9P$
3d	*e*	water−acetone	165−167	$C_{17}H_{18}O_9NaP$
3e	93[g]	ethyl acetate−hexane	164−165	$C_{19}H_{20}O_7$
4a	98	methanol	124−125 (lit.[8] 124−125)	$C_{17}H_{16}O_6$
4b	75	hexane	104−105	$C_{18}H_{20}O_4$
4c	53	toluene−hexane	120−122 (lit.[14] 120.5−121)	$C_{18}H_{20}O_6$
4d	70	hexane	121−122	$C_{18}H_{20}O_6$
4e	34	hexane	131−132	$C_{16}H_{14}Cl_2O_4$
4f	36	hexane	121−123	$C_{16}H_{14}F_2O_4$

[a] Crystallized following concentration of the flash column chromatography solvent. [b] Crystallized at 0 °C upon isolation. [c] All compounds were subjected to combustion analysis for C and H (and for Cl, F, and N where appropriate). The results were within ±0.4% of the calculated values. The ^1H and ^{13}C NMR data at 300 MHz were also consistent with the assigned structure. [d] From **3b**. [e] From **3c**. [f] Percent yield from acid chloride. [g] Percent yield from phenstatin.

Scheme 3

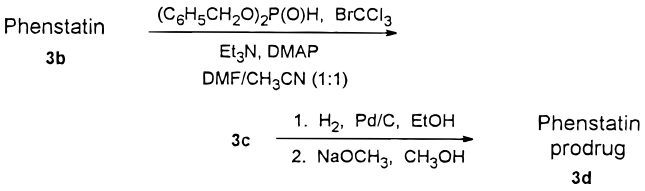

Table 2. Comparative Evaluations of Phenstatin (**3b**), Phenstatin Prodrug (**3d**), Combretastatin A-4 Prodrug (**1d**), and Other Related Benzophenones (**4a**−**f**) in the NCI 60 Cell Line Human Tumor Screen[a]

compd	mean panel GI_{50} (±SD)[b] ($\times 10^{-8}$ M)	COMPARE correlation coefficient[b]
3b	6.01 (3.76)	1.00
3d	7.33 (4.54)	0.94
1d	1.28 (0.44)	0.81
4a	270 (21.4)	0.74
4b	348 (45.4)	0.79
4c	511 (52.5)	0.74
4d	54.3 (4.94)	0.80
4e	512 (69.8)	0.73
4f	494 (99.0)	0.75

[a] Compounds were tested in triplicate in the NCI screen as described[17,20,21] in each of three concentration ranges (HITEST[20] 10^{-5}, 10^{-6}, and 10^{-7} M) using five, 10-fold dilutions within each range. [b] Descriptions and methods of calculation are described elsewhere.[20] COMPARE analyses were performed using the mean graph profiles[20] of phenstatin (**3b**) as the seed.

Consistent with the relative antiproliferative activities summarized in Table 4, phenstatin (**3b**) was equivalent to combretastatin A-4 (**1b**) in its interactions with tubulin in the assays used here. Confirming unpublished observations with other bulky substituents on the B-ring hydroxyl, the combretastatin prodrug (**1d**) was totally inactive against purified tubulin, but, unexpectedly, the phenstatin prodrug (**3d**) had weak activity in inhibiting assembly and moderate activity as an inhibitor of colchicine binding. In the latter assay the prodrug was about 40% as active as phenstatin.

Previous structure−activity studies[3f,g,h] had demonstrated maximal activity with tubulin with a 2-carbon bridge in the (*Z*)-stilbene configuration, whether or not the B-ring hydroxyl was present, and the data of Table 4 reiterate this conclusion. The tetramethoxy ketone **3f** has shown increased activity relative to the analogous diphenylmethane **7b**,[3f] but the recovery of activity versus the (*Z*)-stilbene **1e** was incomplete. In contrast,

Table 3. Comparative Murine P388 Lymphocytic Leukemia Cell Line and Human Cancer Cell Growth Inhibition for Phenstatin (**3b**) vs the Phenstatin Prodrug (**3d**) and Combretastatin A-4 Prodrug (**1d**)

		GI_{50} μg/mL		
cell type	cell line	phenstatin (**3b**)	phenstatin prodrug (**3d**)	combretastatin A-4 prodrug (**1d**)
leukemia	P388	0.0033	<0.001	0.0004
ovarian	OVCAR-3	0.0023	0.0025	0.023
CNS	SF-295	0.052	0.012	0.036
renal	A498	0.38	0.05	0.041
lung-NSC	NCI-H460	0.0057	0.035	0.029
colon	KM20L2	0.04	0.27	0.34
melanoma	SK-MEL-5	0.0038	0.0047	0.041

Table 4. Inhibition of Tubulin Polymerization and Colchicine Binding by Phenstatin, Combretastatin A-4, and Related Compounds[a]

compd	inhibition of tubulin polymerization, IC_{50} (μM ± SD)[b]	inhibition of colchicine binding (% inhibition)
1b	1.2 ± 0.1	97
1d	>80	4
1e	1.3 ± 0.2	97
3b	1.0 ± 0.2	86
3d	21 ± 3	37
3e	3.5 ± 0.5	71
4a	15 ± 2	0
4b	11 ± 2	7
4c	15 ± 2	1
4d	3.6 ± 0.8	58
4e	36 ± 6	1
4f	39 ± 7	0
7a	3.3 ± 0.5	65
7b	4.4 ± 0.2	56
8a	2.1 ± 0.3	77
8b	3.2 ± 0.3	54

[a] Reaction conditions described in detail in the Experimental Section. [b] SD, standard deviation.

in the presence of the B-ring hydroxyl, the reduced activity of the diphenylmethane **7a** was completely recovered in the ketone phenstatin (**3b**).

In terms of the effect of the B-ring hydroxyl on interactions with tubulin, no significant difference was observed between the (*Z*)-stilbenes (**1b**,**e**), slight differences were seen between the diphenylmethanes (**7a**,**b**) and the dibenzyls (**8a**,**b**), and a small difference was observed between the ketones (**3b**,**f**). When a difference was observed, it was always the phenol that had the greater activity.

Manipulation of molecular models demonstrated that it was possible to closely superimpose the two phenyl rings in the ketones with those in the (*Z*)-stilbenes, but this was also possible with the bibenzyls. This may indicate that tubulin specifically recognizes the sp^2 hybridization introduced with the carbonyl and stilbene bridges or the ring conjugation, analogous to that in colchicine, that these two bridges permit. The greater activity of **3b** relative to **3f** may also indicate that the B-ring phenol group imposes steric constraints on the relative positions of the two phenyl rings.

The series of substituent modifications represented by compounds **4a**−**f** failed to yield a derivative superior to **3b** as an inhibitor of either cell growth or tubulin polymerization. Compound **4a**, which is closely analogous to the A, B, and E rings of podophyllotoxin (**5**), had only weak activity against tubulin, and this was comparable to that obtained with **4c**. Compound **4c** has vicinal methoxy groups, with the hydroxyl group of **3b** replaced by a methoxy group, instead of the methylenedioxy bridge of **4a**. The best activity in this group of compounds was observed with di-*m*-methoxy groups in ring B (**4d**), but this compound was 3−4-fold less potent than phenstatin in inhbiting tubulin polymerization. There was a further 3-fold drop in activity with di-*m*-methyl groups in ring B (**4b**), and compounds with halogens at these positions (**4e**,**f**) were almost inert with tubulin. In the presence of a *p*-methoxy group, the bulkiness of the substituent and/or the presence of an oxygen in the *meta*-position of ring B seems to be critical for optimum inhibitory activity against tubulin in the ketone derivatives. A hydrogen (**3f**) leads to greater inhibition than a methoxy or phosphate group (**4c, 3d**) but is less effective than a hydroxyl (**3b**).

On the basis of the ring substituent structural modifications of phenstatin described herein, both the sp^2 hybridization of the carbonyl carbon that preserves the relative *cis*-relationship of the aromatic rings and the specific 3-hydroxy-4-methoxy substitution appear necessary for strong cancer cell growth inhibition. Further development of phenstatin and its prodrug is in progress.

Experimental Section

General Experimental Procedures. Ether (anhydrous diethyl ether), tetrahydrofuran (distilled from sodium and benzophenone), thionyl chloride, and morpholine were distilled prior to use. Reagents were obtained from Sigma−Aldrich Co. Solvent extracts of aqueous solutions were dried over anhydrous magnesium sulfate unless otherwise noted. Flash column chromatography was performed using silica gel (230−400 mesh) and hexanes−ethyl acetate as eluant. Analtech silica gel GHLF plates were used for TLC. All compounds were visible with fluorescent short-wave light (254 nm).

Melting points were recorded employing an Electrothermal 9100 apparatus and are uncorrected. ^{1}H and ^{13}C NMR spectra were recorded by means of a Varian VXR-300 instrument and referenced to chloroform. ^{31}P NMR was obtained from a Varian VXR-500 and referenced to an external standard (85% aqueous H_3PO_4). Mass spectral data were recorded using a Varian MAT 312 instrument (EIMS), and IR spectra were determined with a Mattonson Instruments 2020 Galaxy Series FTIR instrument. X-ray crystal structure data collection was performed on an Enraf-Nonius CAD4 diffractometer.

Jacobsen Oxidation of Combretastatin A-4 (1b). To a mixture of 4-phenylpyridine *N*-oxide (0.127 g, 0.74 mmol) and (*R*,*R*)-(−)-[*N*,*N*^{1}-bis(3,5-di-*tert*-butylsalicylidene)-1,2-cyclohexanediaminoat(2−)]manganese(III) chloride[6b] (0.024 g, 0.037 mmol) in a 50-mL flask was added a solution of 3′-[(*tert*-butyldimethylsilyl)oxy]combretastatin A-4 (**1c**; 0.80 g, 1.86 mmol) in 3 mL of ethyl acetate (or methylene chloride). The mixture was stirred at 4 °C for 20 min followed by addition of an aqueous 0.50 M NaOCl solution (6.32 mL, 3.16 mmol) via syringe. The temperature remained at 4 °C, and reaction progress was monitored by TLC (4:1 hexanes−EtOAc). After 5 h, the reaction mixture was warmed to room temperature and the aqueous phase removed. The organic layer was washed successively with water (2 × 10 mL) and brine (10 mL) and dried over anhydrous Na_2SO_4. Filtration and solvent removal in vacuo gave a brown residue that was subjected to flash column chromatography (4:1 hexanes−ethyl acetate, 1-in. × 12-in. column). The silyl ether-protected benzophenone **3a** (R_f = 0.27) was collected as a yellow oil. A second flash column chromatographic separation was necessary for final purification. Consistent 10% yields were obtained based on conversion of combretastatin A-4 silyl ether to phenstatin (**3b**; see below).

Phenstatin (3b). Silyl ether **3a** (4.90 g, 11.3 mmol) was dissolved in dry tetrahydrofuran (100 mL), and 1.0 M tetrabutylammonium fluoride (11.3 mL, 11.3 mmol) was added (slowly via syringe) while rapidly stirring under Ar.[5] After 15 min, ice (20 g) and ether (100 mL) were added successively. The ethereal layer was washed with water (3 × 100 mL), dried, and filtered, and solvent was removed under reduced pressure to yield a yellow solid. Flash chromatography (eluant: 3:2 hexanes−ethyl acetate, R_f = 0.17) was performed and afforded an off-white solid that recrystallized from hexane as colorless granules: EIMS *m*/*z* (peak height) 318 (M^+, 100), 303 (14), 195 (30), 151 (36). IR (Nujol, cm^{-1}) 1633 (C═O), 1604 (aromatic C═C); ^{1}H NMR ($CDCl_3$) δ 7.406 (1H, dd, $J_{6/2}$ = 2.1 Hz, $J_{6/5}$ = 9.4 Hz, H-6), 7.362 (1H, d, $J_{2/6}$ = 2.1 Hz, H-2), 7.011 (2H, s, H-2′,6′), 6.906 (1H, d, $J_{5/6}$ = 8.4 Hz, H-5), 5.662 (1H, s, −OH), 3.969 (3H, s, 4′-OCH_3), 3.913 (3H, s, 4-OCH_3), 3.860 (6H, s, 3′,5′-OCH_3); ^{13}C NMR (75.5 MHz, $CDCl_3$, assignments deduced with assistance from an APT spectrum) δ 193.3 (C═O), 152.8 (C-3′,5′), 150.2 (C-4), 145.3 (C-3), 141.7 (C-4′), 133.2 (C-1′), 131.1 (C-1), 123.6 (C-6), 116.2 (C-2), 110.0 (C-5), 107.5 (C-2′,6′), 60.9 (4-OCH_3), 56.3 (3′,5′-OCH_3), 56.1 (4′-OCH_3).

Phenstatin Acetate (3e). Acetic anhydride (74 μL, 0.79 mmol) was added to a solution of phenstatin (**3b**; 0.2 g, 0.63 mmol), DMAP (7.8 mg, 0.063 mmol), and triethylamine (0.13 mL, 0.94 mmol) in dry methylene chloride (1.5 mL) under argon at room temperature. The yellow solution was stirred for 30 min (reaction was complete by TLC). Methanol (5 mL) was added and the reaction mixture concentrated to a solid that was washed with diethyl ether (3 × 10 mL) and partitioned between ethyl acetate and cold l N hydrochloric acid. The organic layer was washed with 10% aqueous sodium bicarbonate and dried. Solvent removal, in vacuo, gave an off-white solid that was recrystallized from ethyl acetate−hexane to give colorless snowflakes of analytical purity: EIMS *m*/*z* (peak height) 360 (M^+, 60), 318 (100), 303 (10), 195 (20), 151 (30), 91 (32), 44 (25); ^{1}H NMR ($CDCl_3$) δ 7.740 (1H, dd, $J_{6/2}$ = 2.1 Hz, $J_{6/5}$ = 8.1 Hz, H-6), 7.556 (1H, d, $J_{2/6}$ = 2.1 Hz, H-2), 7.026 (1H, d, $J_{5/6}$ = 8.0 Hz, H-5), 7.013 (2H, s, H-2′,6′), 3.914 (3H, s, 4-OCH_3), 3.907 (3H, s, 4′-OCH_3), 3.863 (6H, s, 3′,5′-OCH_3), 2.315 (3H, s, −$OCOCH_3$).

X-ray Crystal Structure Determination of Phenstatin (3b). Colorless crystals of ketone **3b** were grown as clusters of thick plates from an ether solution. Cleavage of a single-crystal fragment from one of the clusters provided a usable

specimen (0.54 × 0.32 × 0.28 mm), which was mounted on the end of a glass capillary tube. Data collection was performed at 25 ± 1 °C. Crystal data: $C_{17}H_{18}O_6$, monoclinic space group $P2_1/c$ with $a = 12.608(2)$, $b = 14.858(2)$, and $c = 8.738(3)$ Å, $\beta = 104.69(2)°$, $V = 1583.3(12)$ Å^3, λ(Cu Kα) = 1.541 78 Å, $\rho_0 = 1.299$ g cm^{-3}, $\rho_c = 1.335$ g cm^{-3} for $Z = 4$ and FW = 318.31, $F(000) = 672$. All reflections corresponding to slightly more than a complete quadrant, with $2\Theta \leq 130°$, were measured using the $\omega/2\Theta$ scan technique. After Lorentz and polarization corrections, merging of equivalent reflections and rejection of systematic absences, 2610 unique reflections remained, of which 2453 were considered observed ($I_o > 2\sigma(I_o)$) and were used in the subsequent refinement. Linear and anisotropic decay corrections were applied to the intensity data, as well as an empirical absorption correction (based on a series of psi-scans).[22] Structure determination was accomplished with the direct-methods program SIR92.[23] All nonhydrogen atoms were located on the first run of SIR92, using the default settings. The H atom coordinates, calculated at optimum positions and added in the final stages of least-squares refinement, were forced to ride the atom to which they were attached but were not refined. The final cycle of refinement included 209 variable least-squares parameters (anisotropic refinement on all non-hydrogen atoms). The structure determined for **3b** converged to the standard crystallographic residual of $R_1 = 0.0462$ for 2453 reflections in which $F_o > 4.0\ \sigma(F_o)$ and 0.0480 for all 2610 reflections. The corresponding wR_2 Sheldrick values, based on F_o^2, were 0.1454 and 0.1475, respectively. The goodness of fit for all data was 1.042. Final bond distances and angles were all within acceptable limits. The final difference Fourier map showed minimal residual electron density with the highest difference peak corresponding to 0.20 e/Å^3. A computer-generated perspective drawing of **3b** is shown in Figure 1.[24]

3-[(*tert*-Butyldimethylsilyl)oxy]-4-methoxybenzoic Acid. To a solution of 3-[(*tert*-butyldimethylsilyl)oxy]-4-methoxybenzaldehyde[2] (35.0 g, 131 mmol) in acetone (400 mL) was added (stirring) a warm solution (40 °C) of potassium permanganate (35.3 g, 223 mmol) in water (50 mL)−acetone (250 mL) over 30 min. The reaction mixture was stirred for 45 min (complete by TLC analysis). The suspension was cooled and filtered through a pad of Celite, and the filtrate was concentrated. The residue was dissolved in ethyl acetate (1000 mL) and transferred to a separatory funnel containing 1 N HCl (800 mL). The organic layer was extracted with water (5 × 1000 mL) and brine (500 mL) and dried (sodium sulfate), and solvent was removed in vacuo to give a crystalline powder. Recrystallization from hexane afforded the benzoic acid as colorless needles (31.0 g, 84% yield): mp = 163.5−164.5 °C; EIMS *m/z* (peak height) 282 (M$^+$), 267 (2), 225 (92), 210 (100), 195 (20); IR (Nujol, cm^{-1}) 3100 (broad O−H stretch), 1682 (C=O), 1681 (aromatic C=C); ^{1}H NMR ($CDCl_3$) δ 7.732 (1H, dd, $J_{6/2} = 2.2$ Hz, $J_{6/5} = 8.4$ Hz, H-6), 7.569 (1H, d, $J_{2/6} = 1.2$ Hz, H-2), 6.894 (1H, d, $J_{5/6} = 8.5$ Hz, H-5), 3.882 (3H, s, $-OCH_3$), 1.009 (9H, s, −OtBu), 0.174 (6H, s, $-Si(CH_2)_2-$); ^{13}C NMR (75.5 MHz, $CDCl_3$, assignments assisted by an APT spectrum) δ 172.9 (C=O), 156.6 (C-4), 145.4 (C-3), 125.7 (C-2), 123.0 (C-6), 122.4 (C-1), 111.5 (C-5), 55.8 ($-OCH_3$), 25.9 ($-CH_3$), −4.5 ($-Si(CH_2)_2-$), −4.5 ($-Si-C-$).

General Procedure for Synthesis of Morpholine Amides 6a−g. To a 1.0 M solution of the carboxylic acid chloroform at room temperature was added 2 equiv of thionyl chloride. The solution was heated to reflux under Ar until TLC (3:1 hexanes−ethyl acetate) showed no starting material (approximately 4−8 h). The solution was concentrated to an oil that solidified under high vacuum (0.05 mmHg), and the crude acid chloride was used in the next step without purification. Two equivalents of morpholine was slowly injected via syringe over a 5-min period to a 0.3 M solution of the acid chloride in toluene (under Ar). The reaction mixture was stirred at room temperature until the starting acid chloride was consumed (approximately 1.5−4 h, according to TLC using 3:1 hexanes−ethyl acetate). The solution was filtered through a pad of Celite to remove morpholine hydrochloride, and the pad washed with toluene. The filtrate was concentrated to an oil that was subjected to flash column chromatography. Concentration of the respective fractions led to the respective amides (Table 1). **6f**,**g** were synthesized from the acid chloride.

***N*-[3-[(*tert*-Butyldimethylsilyl)oxy]-4-methoxybenzoyl]morpholine (6a).** A cottonlike solid was obtained following chromatography (eluant: hexanes−ethyl acetate, 3:2 → 1:4) and recrystallization from hexane (Table 1): EIMS *m/z* (peak height) 351 (M$^+$), 336 (4), 294 (100), 278 (26), 265 (8), 193 (70), 165 (16).

***N*-[3,4-(Methylenedioxy)benzoyl]morpholine (6b).** Amide **6b**[15] was isolated as a colorless flaky solid following chromatography (1:1 hexanes−ethyl acetate, $R_f = 0.22$).

***N*-(3,5-Dimethylbenzoyl)morpholine (6c).** After chromatography (3:2 hexanes−ethyl acetate, $R_f = 0.19$), a fluffy-appearing solid was obtained (Table 1).

***N*-(3,4-Dimethoxybenzoyl)morpholine (6d).** Amide **6d** was obtained as a colorless flaky solid[14] following chromatography (1:2 hexanes−ethyl acetate, $R_f = 0.16$).

***N*-(3,5-Dimethoxybenzoyl)morpholine (6e).** After chromatographic (1:1 hexanes−ethyl acetate, $R_f = 0.18$) purification, amide **6e** was collected as a colorless solid: TOF *m/z* 251.6 (M$^+$).

***N*-(3,5-Dichlorobenzoyl)morpholine (6f).** The clear oily product crystallized at 0 °C: EIMS *m/z* (peak height) 259 (M$^+$), 261 (M + 2), 263 (M + 4), 258 (M$^+$ − H), 175 (62), 173 (96), 86 (76), 56 (100).

***N*-(3,5-Difluorobenzoyl)morpholine (6g).** Amide **6g** (R_f = 0.21 in 3:2 hexanes−ethyl acetate) gave EIMS *m/z* (peak height) 227 (M$^+$), 141 (100), 113 (50), 86 (36), 56 (66).

General Procedures for Synthesis of Benzophenones 3a and 4a−f. A flame-dried flask containing a 0.1 M solution of 3,4,5-trimethoxybromobenzene[9] (1.1 equiv in dry tetrahydrofuran) was cooled to −78 °C, evacuated to 1 Torr, and refilled with Ar for 10 cycles. To this solution was slowly added *tert*-butyllithium (2.2 equiv), and the reaction mixture was stirred for 15 min. A second dry flask containing a 0.1 M solution of the morpholine amide (1.0 equiv) in tetrahydrofuran was cooled to −78 °C, evacuated, and refilled with Ar. The phenyllithium reagent was transferred via cannula to the amide solution. The reaction mixture was stirred at −65 to −78 °C for 4 h, followed by a slow warming to room temperature. Progress of the reaction was monitored by TLC (hexanes−ethyl acetate). The reaction was stopped by adding 6 equiv of isopropyl alcohol and stirring for 1 h. Water was added, and the mixture was extracted with ether (3×). The ethereal extracts were combined, washed with water, and dried, and solvent was removed to give an oil that was subjected to flash chromatography. Collection and concentration of the required fractions afforded the benzophenone (Table 1).

3-[(*tert*-Butyldimethylsilyl)oxy]- 3′,4,4′,5′-tetramethoxybenzophenone (3a). Using amide **6a** (0.20 g, 0.57 mmol), 3,4,5-trimethoxybromobenzene (0.169 g, 0.683 mmol), and *t*-BuLi (0.74 mL, 1.25 mmol), the above scheme led to crude phenstatin silyl ether **3a** (0.199 g, $R_f = 0.29$ in 4:1 hexanes−ethyl acetate). Purification and recrystallization from hexane afforded large glasslike prisms (Table 1): EIMS *m/z* (peak height) 432 (M$^+$), 417 (2), 402 (1), 375 (100), 360 (58), 345 (4), 193 (26).

3,4,5-Trimethoxy-3′,4′-(methylenedioxy)benzophenone (4a). Flash column chromatography (4:1 hexanes−ethyl acetate, $R_f = 0.20$) and recrystallization from methanol afforded small colorless needles.[8]

3,4,5-Trimethoxy-3′,5′-dimethylbenzophenone (4b). Chromatography (9:1 hexanes−ethyl acetate, $R_f = 0.19$) and recrystallization from hexane yielded off-white needles: EIMS *m/z* (peak height) 300 (M$^+$, 100), 285 (14), 270 (4), 375 (100), 195 (40).

3,3′,4,4′,5-Pentamethoxybenzophenone (4c). Purification by column chromatography (4:1 hexanes−ethyl acetate, $R_f = 0.10$) and recrystallization from toluene−hexane gave an off-white powder: EIMS *m/z* (peak height) 332 (M$^+$, 100), 317 (6), 301 (8), 195 (16), 165 (22).

3,3′,4,5,5′-Pentamethoxybenzophenone (4d). After recrystallization from hexane, the off-white powder did not require chromatographic purification: EIMS *m/z* (peak height) 332 (M^+, 100), 317 (6), 301 (8), 195 (16), 165 (22).

3,5-Dichloro-3′,4′,5′-trimethoxybenzophenone (4e). Chromatographic (9:1 hexanes−ethyl acetate, R_f = 0.28) separation and recrystallization from hexane afforded clear diamond-shaped crystals: EIMS *m/z* (peak height) 340 (M^+, 100), 342 (M + 2), 344 (M + 4), 325 (26), 310 (4), 195 (46).

3,5-Difluoro-3′,4′,5′-trimethoxybenzophenone (4f). Following chromatography (9:1 hexanes−ethyl acetate, R_f = 0.21) and recrystallization from hexane, the ketone was obtained as colorless needles: EIMS *m/z* (peak height) 318 (M^+, 100), 293 (20), 278 (4), 195 (22), 141 (36), 113 (16).

3-(*O*-Dibenzylphosphoryl)phenstatin (3c). To a dry flask equipped with a septum, magnetic stirrer, thermometer, and Ar inlet containing dry acetonitrile (50 mL) and DMF (50 mL) was added phenstatin (**3b**; 2.0 g, 6.28 mmol). Upon cooling to −10 °C, bromotrichloromethane (3.10 mL, 31.4 mmol) was added followed by triethylamine (1.84 mL, 13.2 mmol) and (dimethylamino)pyridine (77 mg, 0.63 mmol). After 1 min, dropwise addition of dibenzyl phosphite was begun while maintaining a temperature of −7 to −10 °C. The resultant yellow solution was monitored by TLC (1:1 hexanes−ethyl acetate, R_f = 0.19) until complete. At that time (1.5 h), 0.5 M aqueous KH_2PO_4 (50 mL) was added followed by extraction with ethyl acetate (3 × 100 mL). The organic extract was washed successively with water (200 mL) and brine (150 mL) and dried (sodium sulfate). The solution was filtered and concentrated in vacuo to a milky oil. Flash column chromatography (eluant: 1:1 hexanes−ethyl acetate) was performed to give benzyl phosphate **3c** as a clear oil (2.60 g, 72% yield): EIMS *m/z* (peak height) (578, M^+), (486, 4), (91, 100); ^{1}H NMR ($CDCl_3$) δ 7.694 (1H, d, $J_{6/5}$ = 8.0 Hz, H-6), 7.657 (1H, s, H-2), 7.319 (10H, s, Ar−H), 7.025 (2H, s, H-2′,6′), 7.000 (1H, d, $J_{5/6}$ = 9.0 Hz, H-5), 5.182 (4H, d, J = 8.5 Hz, O−CH_2−Ph), 3.880 (9H, s, 3′,5′,4-OCH_3); ^{31}P NMR ($CDCl_3$, decoupled, 202.35 MHz) δ −5.22.

Disodium Phenstatin 3-*O*-Phosphate (3d). The benzyl phosphate **3c** (0.68 g, 1.18 mmol) was added to anhydrous ethyl alcohol (denatured, 50 mL) in a dry flask equipped with a magnetic stirrer. After the vessel was evacuated and refilled with Ar (two cycles), 5% palladium-on-carbon (0.58 g) was added. The flask was evacuated and refilled with H_2 to 10 psi (3×). The mixture was stirred vigorously for 15 min and filtered through a 1-cm pad of Celite. The flask and Celite were washed with ethanol, and solvent was removed under reduced pressure to afford a foamy tan solid (0.44 g) that was used in the next step.

The deprotected phosphate (0.44 g, 1.10 mmol) was dissolved in anhydrous methanol (15 mL), and sodium methoxide (88 mg, 2.20 mmol) was added at room temperature. The cloudy solution was stirred for 20 h, and the reaction mixture was concentrated to a white solid that was washed with 2-propanol and recrystallized (3×) from water−acetone. The phenstatin prodrug **3d** (0.38 g, 78% yield) was collected by filtration and found to give: LRFAB *m/z* 443.02 (M + H^+), calcd 443.048; EIMS *m/z* (peak height) 318 (100, $M^+ - PO_3Na_2 + H$), 303 (12), 195 (20), 151 (23); ^{1}H NMR (D_2O) δ 7.644 (1H, t, $J_{2/6}$ = 1.8 Hz, H-2), 7.366 (1H, dd, $J_{6/2}$ = 1.8 Hz, $J_{6/5}$ = 8.5 Hz, H-6), 7.006 (1H, d, $J_{5/6}$ = 8.5 Hz, H-5), 6.933 (2H, s, H-2′,6′), 3.844 (3H, s, 4′-OCH_3), 3.748 (6H, s, 3′,5′-OCH_3) 3.734 (3H, s, 4-OCH_3); ^{13}C NMR (D_2O, reference to $CDCl_3$) δ 193.5 (C═O), 151.1; ^{31}P NMR (D_2O, decoupled, −202.35 MHz) δ −1.965. The solubility of phenstatin prodrug **3d** was found to be 30 mg/mL in distilled water at 25 °C.

Tubulin Assays. Electrophoretically homogeneous bovine brain tubulin was purified from bovine brain as described previously.[25] Reaction mixtures (0.24 mL during preincubatin, 0.25 mL during incubation, with all concentrations referring to the final volume) contained 0.8 M monosodium glutamate (taken from 2.0 M stock solution adjusted to pH 6.6 with HCl), 1.0 mg/mL (10 μM) tubulin, 4% (v/v) dimethyl sulfoxide, and varying concentrations of drug. Samples were incubated for 15 min at 30 °C and chilled on ice. GTP, required for polymerization, was added in 10 μL to a final concentration of 0.4 mM. Samples were transferred to cuvettes held at 0 °C by electronic temperature controllers in Gilford model 250 recording spectrophotometers. Baselines were established, and the reaction was initiated by a jump (approximately 1 min) to 30 °C. Extent of assembly after 20 min was the parameter used to determine IC_{50} values. Active compounds were examined in at least three independent experiments, and inactive compounds were generally evaluated twice. In most experiments, four spectrophotometers were used, with two control reaction mixtures.

The binding of [^{3}H]colchicine to tubulin was measured on DEAE-cellulose filters as described elsewhere.[26] Reaction mixtures contained 0.1 mg/mL (1.0 μM) tubulin, 5.0 μM [^{3}H]-colchicine, and 5.0 μM inhibitor and were incubated for 10 min at 37 °C.

Acknowledgment. Appreciation and thanks for support of this research are extended to the following: Outstanding Investigator Grant CA 44344-05-9 with the Division of Cancer Treatment, Diagnosis and Centers, NCI, DHHS; the Arizona Disease Control Research Commission; Virginia Piper; Diane Cummings Halle; Rod and Hazel McMullen; Gary L. and Diane Tooker; Polly Trautman; John and Edith Reyno; and the Robert B. Dalton Endowment. We are thankful for the assistance of Drs. Jean-Charles Chapuis, Cherry L. Herald, Fiona Hogan, Jean M. Schmidt, and Michael D. Williams, as well as David M. Carnell and Lee Williams, the National Science Foundation for equipment Grant CHE-8409644, and the NSF Regional Instrumentation Facility in Nebraska (Grant CHE-8620177).

Supporting Information Available: X-ray crystallographic tables of atomic coordinates, bond lengths and angles, and anisotropic thermal parameters for **3b** (6 pages). Ordering information is given on any current masthead page.

References

(1) (a) For contribution 378, see: Pettit, G. R.; Bond, T. J.; Herald, D. L.; Penny, M. G.; Doubek, D. L.; Williams, M. D.; Tackett, L. P.; Hooper, J. N. A. Isolation and Structure of Spongilipid from the Republic of Singapore Marine Poriferan *Spongia cf. Hispida*. *Can. J. Chem.* **1997**, **75**, 920−925. (b) Laboratory of Drug Discovery Research and Development, Developmental Therapeutics Program, Division of Cancer Treatment, Diagnosis and Centers, National Cancer Institute, Frederick Cancer Research Development Center, Frederick, MD 21702-1201.

(2) (a) Pettit, G. R.; Singh, S. B.; Boyd, M. R.; Hamel, E.; Pettit, R. K.; Schmidt, J. M.; Hogan, F. Antineoplastic Agents 291. Isolation and Synthesis of Combretastatins A-4, A-5, and A-6. *J. Med. Chem.* **1995**, *38*, 1666−1672. (b) Hamel, E. Antimitotic Natural Products and Their Interactions with Tubulin. *Med. Res. Rev.* **1996**, *16*, 207−231.

(3) (a) Bedford, S. B.; Quarterman, C. P.; Rathbone, D. L.; Slack, J. A.; Griffin, R. J.; Stevens, M. F. G. Synthesis of Water-Soluble Prodrugs of the Cytotoxic Agent Combretastatin A-4. *BioMed. Chem. Lett.* **1996**, *6*, 157−160. (b) Medarde, M.; Pelaez-Lamamié de Clairac, R.; Ramos, A. C.; Caballero, E.; López, J. L.; Grávalos, D. G.; San Feliciano, A. Synthesis and Pharmacological Activity of Combretastatin Analogues, Naphthylcombretastatins and Related Compounds. *BioMed. Chem. Lett.* **1995**, *5*, 229−232. (c) Li, L.; Wang, H.-K.; Kuo, S.-C.; Wu, T.-S.; Mauger, A.; Lin, C. M.; Hamel, E.; Lee, K.-H. Antitumour Agents 155. Synthesis and Biological Evaluation of 3′,6,7-Substituted 2-Phenyl-4-quinolones as Antimicrotubule Agents. *J. Med. Chem.* **1994**, *37*, 3400−3407. (d) Mannila, E.; Talvitie, A. Combretastatin Analogues via Hydration of Stilbene Derivatives. *Liebigs Ann. Chem.* **1993**, 1037−1039. (e) Cushman, M.; He, H.-M.; Lin, C. M.; Hamel, E. Synthesis and Evaluation of a Series of Benzylaniline Hydrochlorides as Potential Cytotoxic and Antimitotic Agents Acting by Inhibition of Tubulin Polymerization. *J. Med. Chem.* **1993**, *36*, 2817−2821. (f) Cushman, M.; Nagarathnam, D.; Gopal, D.; He, H.-M.; Lin, C. M.; Hamel, E. Synthesis and Evaluation of Analogues of (*Z*)-1-(4-Methoxyphenyl)-2-(3,4,5-trimethoxyphenyl)ethene as Potential Cytotoxic and Antimitotic Agents. *J. Med. Chem.* **1992**, *35*, 2293−2306. (g) Getahun, Z.; Jurd, L.; Chu,

P. S.; Lin, C. M.; Hamel, E. Synthesis of Alkoxy-Substituted Diaryl Compounds and Correlation of Ring Separation with Inhibition of Tubulin Polymerization: Differential Enhancement of Inhibitory Effects under Suboptimal Polymerization Reaction Conditions. *J. Med. Chem.* **1992**, *35*, 1058−1067. (h) Cushman, M.; Nagarathnam, D.; Gopal, D.; Chakraborti, A. K.; Lin, C. M.; Hamel, E. Synthesis and Evaluation of Stilbene and Dihydrostilbene Derivatives as Potential Anticancer Agents That Inhibit Tubulin Polymerization. *J. Med. Chem.* **1991**, *34*, 2579−2588. (i) Couladouros, E. A.; Soufli, I. C. Total Synthesis of Natural (−)-Combretastatin D-1. *Tetrahedron Lett.* **1995**, *51*, 9369−9372.

(4) (a) Kitanaka, S.; Takido, M.; Mizoue, K.; Kondo, H.; Nakaike, S. Oligomeric Stilbenes from *Caragana chamlagu* LAMARK Root. *Chem. Pharm. Bull.* **1996**, *44*, 565−567. (b) Ruby, A. J.; Kuttan, G.; Dinesh Babu, K.; Rajasekharan, K. N.; Kuttan, R. Anti-tumour and Antioxidant Activity of Natural Curcuminoids. *Cancer Lett.* **1995**, *94*, 79−83.

(5) Pietikäinen, P. Asymmetric Epoxidation of Unfunctionalized Alkenes with Periodates Catalyzed by Chiral (Salen) Mn (III) Complexes. *Tetrahedron Lett.* **1995**, *36*, 319−322.

(6) (a) Popisil, P. J.; Carstern, D. H.; Jacobsen, E. N. X-Ray Structural Studies of Highly Enantioselective Mn(salen) Epoxidation Catalysts. *Chem. Eur. J.* **1996**, *2*, 974−980. (b) Palucki, M.; Popisil, P. J.; Zhang, W.; Jacobsen, E. N. Highly Enantioselective, Low-Temperature Epoxidation of Styrene. *J. Am. Chem. Soc.* **1994**, *116*, 9333−9334. (c) Quan, R. W.; Li, Z.; Jacobsen, E. N. Enantiofacially Selective Binding of Prochiral Olefins to a Chiral Catalyst via Simultaneous Face-Face and Edge-Face Aromatic Interactions. *J. Am. Chem. Soc.* **1996**, *118*, 8156−8157. (d) Brandes, B. D.; Jacobsen, E. N. Highly Enantioselective, Catalytic Epoxidation of Trisubstituted Olefins. *J. Org. Chem.* **1994**, *59*, 4378−4380. (e) Chang, S.; Heid, R. M.; Jacobsen, E. N. Enantioselective Epoxidation of Cyclic 1,3-Dienes Catalyzed by a Sterically and Electronically Optimized (Salen) Mn Complex. *Tetrahedron Lett.* **1994**, *35*, 669−672. (f) Chang, S.; Galvin, J. M.; Jacobsen, E. N. Effect of Chiral Quaternary Ammonium Salts on (salen) Mn-Catalyzed Epoxidation of cis-Olefins. A Highly Enantioselective, Catalytic Route to Trans-Epoxides. *J. Am. Chem. Soc.* **1994**, *116*, 6937−6938. (g) Jacobsen, E. N.; Deng, L.; Furukawa, Y.; Martinez, L. E. Enantioselective Catalytic Epoxidation of Cinnamate Esters. *Tetrahedron* **1994**, *50*, 4323−4334. (h) Chang, S.; Lee, N. H.; Jacobsen, E. N. Regio- and Enantioselective Catalytic Epoxidation of Conjugated Polyenes. Formal Synthesis of LTA_4 Methyl Ester. *J. Org. Chem.* **1993**, *58*, 6939−6941. (i) Larrow, J. F.; Jacobsen, E. N.; Gao, Y.; Hong, Y.; Nie, X.; Zepp, C. M. A Practical Method for the Large-Scale Preparation of [*N*,*N*′-Bis(3,5-di-*tert*-butylsalicylidene)-1,2-cyclohexanediaminato(2-)]manganese(III) Chloride, a Highly Enantioselective Epoxidation Catalyst. *J. Org. Chem.* **1994**, *59*, 1939−1942. (j) Yamada, T.; Imagawa, K.; Nagata, T.; Mukaiyama, T. Enantioselective Epoxidation of Unfunctionalized Olefins with Molecular Oxygen and Aldehyde Catalyzed by Optically Active Manganese(III) Complexes. *Chem. Lett.* **1992**, 2231−2234. (k) Takai, T.; Hata, E.; Yorozu, K.; Mukaiyama, T. Cobalt(II) Complex Catalyzed Epoxidation of Olefins by Conbined Use of Molecular Oxygen and Cyclic Ketones. *Chem. Lett.* **1992**, 2077−2080. (l) Irie, R.; Ito, Y.; Katsuki, T. Catalytic epoxidation with Molecular Oxygen Using Nickel Complex. *Tetrahedron Lett.* **1991**, *32*, 6891−6894. (m) Jacobsen, E. N.; Zhang, W.; Muci, A. R.; Ecker, J. R.; Deng, L. Highly Enantioselective Epoxidation Catalysts Derived from 1,2-Diaminocyclohexane. *J. Am. Chem. Soc.* **1991**, *113*, 7063−7064.

(7) (a) Cope, A. C.; Trumbull, P. A.; Trumbull, E. R. Base-catalyzed Rearrangement of Epoxides. *J. Am. Chem. Soc.* **1958**, *80*, 2844−2848. (b) Parker, R. E. Mechanisms of Epoxide Reactions. *Chem. Rev.* **1959**, *59*, 737−799. (c) Alper, H.; Des Roches, D.; Durst, T.; Legault, R. Molybdenum Hexacarbonyl Catalyzed Rearrangement of Epoxides. *J. Org. Chem.* **1976**, *41*, 3611−3613. (d) Bornstein, J.; Joseph, M. A.; Shields, J. E. Solvolyses of 1,1-Diphenyl-2-haloethanols and of 1,1-Diphenylethylene Oxide: Thermal Behavior of the Epoxide and Its Reactions with Phenylmagnesium Bromide and with Phenyllithium. *J. Org. Chem.* **1965**, *30*, 801−807. (e) Thummel, R. P.; Rickborn, B. Stereochemistry of the Base-Induced Rearrangement of Epoxides to Allylic Alcohols. *J. Am. Chem. Soc.* **1970**, *92*, 2064−2067.

(8) Pettit, G. R.; Baumann, M. F.; Rangammal, K. N. Antineoplastic Agents. V. The Aromatic System of Podophyllotoxin (Part B). *J. Med. Pharm. Chem.* **1962**, *5*, 800−808.

(9) Jung, M. E.; Yuk-Sun Lam, P.; Mansuri, M. M.; Speltz, L. M. Stereoselective Synthesis of an Analogue of Podophyllotoxin by an Intramolecular Diels−Alder Reaction. *J. Org. Chem.* **1985**, *50*, 1087−1105.

(10) Pettit, G. R.; Temple, C., Jr.; Narayanan, V. L.; Varma, R.; Simpson, M. J.; Boyd, M. R.; Rener, G. A.; Bansal, N. Antineoplastic Agents 322. Synthesis of Combretastatin A-4 Prodrugs. *Anticancer Drug Des.* **1995,** *10*, 299−309.

(11) Pettit, G. R.; Singh, S. B.; Hamel, E.; Lin, C. M.; Alberts, D. S.; Garcia-Kendall, D. Isolation and Structure of the Strong Cell Growth and Tubulin Inhibitor Combretastatin A-4. *Experentia* **1989**, *45*, 209−211.

(12) Pettit, G. R.; Freeman, S.; Simpson, M. J.; Thompson, M. A.; Boyd, M. R.; Williams, M. D.; Pettit, G. R., III; Doubek, D. L. Antineoplastic Agents 320. Synthesis of a Practical Pancratistatin Prodrug. *Anticancer Drug Des.* **1995**, *10*, 243−250.

(13) Silverberg, L. J.; Dillon, J. L.; Vemishetti, P. A Simple, Rapid and Efficient Protocol for the Selective Phosphorylation of Phenols with Dibenzyl Phosphite. *Tetrahedron Lett.* **1996**, *37*, 771−774.

(14) Gardner, J. A. F.; MacDonald, B. F.; MacLean, J. The Polyoxyphenols of Western Red Cedar (Thuja Plicata Donn). *Can. J. Chem.* **1960**, *38*, 2387−2394.

(15) Kasztreiner, E.; Borsey, J.; Vargha, L. Synthesis and Pharmacological Investigation of New Alkoxybenzamides II. *Biochem. Pharmacol.* **1962**, *11*, 651−657.

(16) Boyd, M. R. Status of the NCI Preclinical Antitumour Drug Discovery Screen. Implications for Selection of New Agents for Clinical Trial. In *CANCER: Principles and Practices of Oncology Updates*; DeVita, V. T., Jr., Hellman, S., Rosenberg, S. A., Eds.; Lippincott: Philadelphia, 1989; Vol. 10, No. 3, pp 1−12.

(17) Boyd, M. R. The Future of New Drug Development. Section I. Introduction to Cancer Therapy. In *Current Therapy in Oncology*; Niederhuber, J. E., Ed.; B. C. Decker, Inc.: Philadelphia, 1993; pp 11−22.

(18) Boyd, M. R.; Paull, K. D.; Rubinstein, L. R. Data Display and Analysis Strategies from NCI Disease-Oriented in Vitro Antitumour Drug Screen. In *Cytotoxic Anticancer Drugs: Models and Concepts for Drug Discovery and Development*; Valeriote, F. A., Corbett, T., Baker, L., Eds.; Kluwer Academic Publishers: Amsterdam, 1992; pp 11−34.

(19) Stinson, S. F.; Alley, M. C.; Kopp, W. C.; Fiebig, H.-H.; Mullendore, L. A.; Pittman, A. F.; Kenney, S.; Keller, J.; Boyd, M. R. Morphological and Immunocytochemical Characteristics of Human Tumor Cell Lines for Use in a Disease-Oriented Anticancer Drug Screen. *Anticancer Res.* **1992**, *12*, 1035−1054.

(20) Boyd, M. R.; Paull, K. D. Some Practical Considerations and Applications of the NCI in Vitro Drug Discovery Screen. *Drug Dev. Res.* **1995**, *34*, 91−109.

(21) Weinstein, J. N.; Myers, T. G.; O′Connor, P. M.; Friend, S. H.; Fornance, A. J.; Kohn, K. W.; Fojo, T.; Bates, S. E.; Rubinstein, L. V.; Anderson, N. L.; Buolamwini, J. K.; van Osdol, W. W.; Monks, A. P.; Scudiero, D. A.; Sausville, E. A.; Zaharevitz, D. W.; Bunow, B.; Viswanadhan, V. N.; Johnson, G. S.; Wittes, R. E.; Paul, K. D. An Information-Intensive Approach to the Molecular Pharmacology of Cancer. *Science* **1997**, *275*, 343−349.

(22) North, A. C.; Phillips, D. C.; Matthews, F. S. A Semiempirical Method of Absorption Correction. *Acta Crystallogr.* **1968**, *A24*, 351−359.

(23) Altomare, A.; Cascarano, G.; Giacovazzo, C.; Guigliardi, A.; Mburla, M.; Polidori, G.; Camalli, M. SIR92 − A Program for Automatic Solution of Crystal Structures by Direct Methods; Dipartimento Geomineralogico, University of Bari, Italy.

(24) Preparation of Figure 1 was done with SHELXTL-PLUS, G. Sheldrick, Siemens Analytical X-Ray Instruments, Inc., Madison, WI 53719.

(25) Hamel, E.; Lin, C. M. Separation of Active Tubulin and Microtubule-Associated Proteins by Ultracentrifugation and Isolation of a Component Causing the Formation of Microtubule Bundles. *Biochemistry* **1984**, *23* (3), 4173−4184.

(26) Kang, G.-J.; Getahun, Z.; Muzaffar, A.; Brossi, A.; Hamel, E. *N*-Acetylcolchinol *O*-Methyl Ether and Thiocolchicine, Potent Analogues of Colchicine Modified in the C Ring: Evaluation of the Mechanistic Basis for Their Enhanced Biological Properties. *J. Biol. Chem.* **1990**, *265*, 10255−10259.

JM970644Q